ELSEVIER

Journal of Molecular Catalysis A: Chemical 158 (2000) 237–249

JOURNAL OF MOLECULAR CATALYSIS A: CHEMICAL

www.elsevier.com/locate/molcata

Catalytic reduction of nitrate and nitrite ions by hydrogen: investigation of the reaction mechanism over Pd and Pd–Cu catalysts

O.M. Ilinitch [a], L.V. Nosova [a], V.V. Gorodetskii [a], V.P. Ivanov [a], S.N. Trukhan [a], E.N. Gribov [a], S.V. Bogdanov [a], F.P. Cuperus [b,*]

[a] *Boreskov Institute of Catalysis, Novosibirsk 630090, Russia*

[b] *Stratingh Institute of Chemistry and Chemical Engineering, NL-9747 AG Groningen, Netherlands*

Abstract

The catalytic behavior of mono- and bimetallic catalysts with Pd and/or Cu supported over γ-Al_2O_3 in the reduction of aqueous nitrate and nitrite ions by hydrogen was investigated. The composition of the supported metal catalysts was analysed using secondary ion mass spectroscopy (SIMS) and X-ray diffraction (XRD) techniques. Surface enrichment of the bimetallic Pd–Cu particles in copper was revealed. Interactions of NO (possible intermediate in reduction of nitrate and nitrite ions) with H_2 over Pd were studied by thermal desorption spectroscopy (TDS) under high-vacuum conditions. The molecular mechanism of NO_3^- and NO_2^- reduction by H_2 as well as the role of Pd and Cu active sites are discussed.

Keywords: Catalytic reduction; Metal catalyst; Pd; Pd–Cu

1. Introduction

The catalytic reduction of nitrate and nitrite ions in water by hydrogen is being studied by several research groups as a potential means of purification for waters contaminated with the soluble salts of these ions. The substances, harmful at concentrations above 50 mg/l, are increasingly produced by agricultural and industrial activities in different regions of the world. The conversion of nitrate and nitrite ions into nitrogen achieved via catalytic reduction by hydrogen at ambient temperatures makes this reaction one of the most suitable ways for the production of drinking water in areas where the concentration of nitrates and/or nitrites exceeds the admissible limits.

The results available in literature point out two main problems that need to be solved for the reactions to be successfully implemented on a large scale, viz. high intrinsic activity and selectivity of the catalyst, and diffusion limitations of the catalytic performance. Supported palladium and bimetallic palladium–copper cat-

* Corresponding author.

1381-1169/00/$ - see front matter
PII: S1381-1169(00)00070-4

alysts proposed for these reactions by the German researchers [1,2] in addition to N_2 yield ammonium, which concentration in drinking water should be kept at low level. The solution to the second of the abovementioned problems, that of the internal diffusion hindrance, is traditionally sought by using the fine catalyst powder in a slurry reactor.

This paper continues our work on the reduction of nitrates and nitrites by hydrogen in a catalytic membrane reactor, where the latter is applied to facilitate the intraporous mass transfer. In the present study the mechanism of nitrate and nitrite ions reduction over Pd-containing catalysts was investigated in an attempt to improve an intrinsic activity and selectivity of the catalytically active component

2. Experimental

2.1. Preparation of catalysts and catalytic membranes

The series of catalysts including γ-Al_2O_3-supported mono- (Pd and Cu) and bimetallic Pd–Cu samples was prepared via (co)impregnation of the support with aqueous solutions of copper nitrate and palladium hydrochloric acid, followed by drying, oxidation and reduction of the impregnated material in an aqueous solution of sodium borohydride ($NaBH_4$) at room temperature. A detailed description of the preparation procedure can be found elsewhere [3]. The metal content was 4.1 wt.% for Pd/Al_2O_3 catalyst and 1.7 wt.% for Cu/Al_2O_3, while the bimetallic $Pd–Cu/Al_2O_3$ catalysts had the fixed palladium loading (ca. 5 wt.%) and a variable copper content (from ca. 1 up to 7 wt.%). The samples of catalytic membrane were prepared via the same procedure. The ceramic membrane developed at Boreskov Institute was employed at this stage as the catalyst support of a specific type. According to the atomic absorption spectroscopy analysis, the catalytic membrane contained 1.6 wt.% of palladium and 1.2 wt.% of copper.

2.2. Characterization techniques

2.2.1. Analysis of the reaction and catalysts

Concentrations of NO_3^- and NO_2^- anions in catalytic experiments were monitored using a liquid ion chromatograph ''Tsvet-3006'' (Russia) with an electroconductivity detector. NH_4^+ cations were analyzed with an ion-selective electrode ELIT-51 (Russia) having 0.6–1400 mg/l linear concentration range. Dispersion and composition of metal particles in the catalysts and membrane were studied by X-ray diffraction (XRD) with an HZG-4C instrument (Freiberger Präzisionmechanik) in CuKα radiation. Metal loadings of the catalysts and the catalytic membrane were determined by atomic absorption spectroscopy (AAS 1N instrument, Carl Zejss-Jena). Other details of the analytical techniques employed in the present study can be found in Ref. [3].

2.2.2. Secondary ion mass spectroscopy (SIMS)

The method is based on the bombardment of a catalyst sample by the beam of high energy Ar^+ ions with a mass-spectral analysis of secondary ions etched out from the sample. The vacuum apparatus equipped with an MC-7201 mass spectrometer (Russia) having a monopol mass analyser sensitive in the range of mass numbers 1–250 was employed. Residual gas pressure in the spectrometer (H_2O, CO and CO_2) did not exceed 3×10^{-6} Pa. The diameter of the primary ion beam incident at an angle of 45° to the normal of the holder surface was 2 mm, resulting in the area of argon bombardment ca. 5 mm^2. The control programs ensured the review analysis of the entire mass spectrum and measurements of ion currents for up to16 masses during the argon bombardment of a sample.

Preparation of the catalyst samples for SIMS study included their rubbing into the high-purity indium (99.999%) wire mesh holder. Argon ions with energy of 4 keV and current density of 0.12 or 0.63 A/m^2 were used for the bombardment of the samples. The thickness of the layer

etched out by the Ar^+ bombardment Z (Å) was determined as suggested in Ref. [4]:

$$Z = 0.06\,JS(A/\rho)t$$

where J is the current density for the primary ions Ar^+ ($\mu A/cm^2$); S the etching coefficient (ca. 2 for the bombardment of Al_2O_3 by Ar^+ ions of 4 keV energy [5,6]); $A = 20.4$, the average atomic mass of the target; $\rho = 3.7$ g/cm^3, the density of the catalyst samples.

In the calculations the etching rate of the metal particles in the catalyst samples was taken to be equal to that of the Al_2O_3 matrix, since the total amount of the metals in the samples was less than 10% [6].

2.2.3. Thermal desorption spectroscopy (TDS)

The experiments were performed in an all-glass ultrahigh vacuum apparatus of 1.5 l volume and base pressure not exceeding 10^{-10} Torr (1 Torr = 133.3 Pa). Palladium wire (99.99% purity) of 0.25 mm diameter with a geometric surface of 1 cm^2 has been used. The gas phase composition was controlled by the omegatrone mass-spectrometer IPDO-2A (Russia). Prior to the thermodesorption experiments, the wire was cleaned of the traces of carbon, sulfur and other contaminations by subsequent cycles of Ar^+ etching, annealing in oxygen and high-temperature annealing in vacuum according to Ref. [7]. The clean palladium surface prepared according to the above procedure was characterized by TDS spectra of H_2, O_2, NO and H_2O that reproduced in detail those reported in the literature [7–10].

TDS spectra were recorded at a constant heating rate of 5 K/s. In order to rule out any contribution of the residual CO ($m/e = 28$ amu) to N_2, ^{15}NO which produces $^{15}N_2$ ($m/e = 30$ amu) was used in the TDS experiments. The technique employed in the present study allowed quantitative analysis of the TDS spectra for H_2, O_2, N_2, N_2O and NO, and qualitative analysis of those for NH_3 and H_2O.

3. Results

3.1. Catalytic reduction of NO_3^- and NO_2^- by H_2 in water over γ-Al_2O_3-supported catalysts

In the experiments performed for the series of γ-Al_2O_3-supported mono- (Pd or Cu) and bimetallic Pd–Cu catalysts (slurry reactor, mean particle size ca. 15 μm) at the conditions where the reaction performance was not affected by the reactants' diffusion [3], the highest catalytic activity in the reduction of an aqueous solution of 200 mg/l $NaNO_3$ was found for the sample with the atomic ratio Pd:Cu = 1:0.8 (Fig. 1). Note that the activity of this catalyst (expressed with respect to the total content of both Pd and Cu in a given sample) is ca. sevenfold higher than that of the Pd/Al_2O_3 sample. If one assigns the catalytic activity exclusively to palladium, the difference in the activity values becomes even more significant.

Selectivities of these catalysts at various NO_3^- conversions towards side products — NO_2^- and NH_4^+ ions — are listed in Table 1. As can be seen, $Pd–Cu/Al_2O_3$ catalysts are significantly

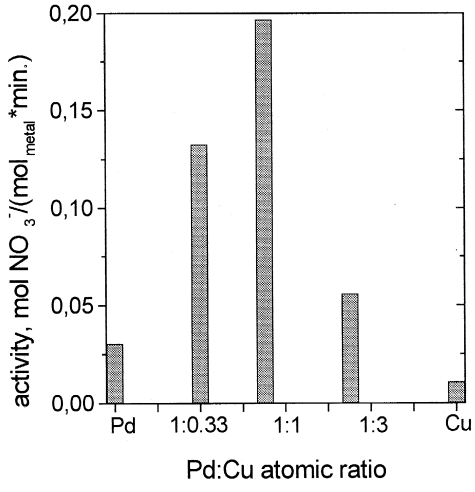

Fig. 1. Activities of Pd/Al_2O_3, Cu/Al_2O_3 and $Pd–Cu/Al_2O_3$ catalysts (mean grain size 15 μm) in reduction of nitrate ions. Reaction conditions: temperature 298 K, $P_{H_2} = 1$ bar, $C_{NO_3^-} = 200$ mg/l, pH = 6.0.

Table 1
Selectivities of Pd/Al_2O_3 and $Pd–Cu/Al_2O_3$ catalysts (mean grain size 15 μm) in reduction of nitrate ions at various NO_3^- conversions
Reaction conditions: temperature 298 K, $P_{H_2} = 1$ bar, $C_{NO_3^-} = 200$ mg/l, pH = 6.0

Atomic ratio of metals in catalyst	$X_{NO_3^-} = 25\%$		$X_{NO_3^-} = 50\%$		$X_{NO_3^-} = 75\%$		$X_{NO_3^-} = 90\%$		$X_{NO_3^-} = 95\%$	
	$S_{NO_2^-}$ (%)	$S_{NH_4^+}$ (%)	$S_{NO_2^-}$ (%)	$S_{NH_4^+}$ (%)	$S_{NO_2^-}$ (%)	$S_{NH_4^+}$ (%)	$S_{NO_2^-}$ (%)	$S_{NH_4^+}$ (%)	$S_{NO_2^-}$ (%)	$S_{NH_4^+}$ (%)
Pd	0	29.0	0	66.0	0	68.0	0	81.0	0	87.0
Pd:Cu = 1:0.33	23.2	11.6	12.5	21.0	5.2	25.0	1.6	31.8	0.9	32.3
Pd:Cu = 1:0.8	22.3	8.6	18.2	10.3	14.0	19.5	7.1	23.9	5.0	24.8
Pd:Cu = 1:2.25	38.0	10.3	43.2	13.4	31.0	17.0	22.9	21.8	17.8	24.3

superior to Pd/Al_2O_3 with respect to much lower selectivity towards NH_4^+. Within the group of $Pd–Cu/Al_2O_3$ catalysts the selectivities for ammonium are about the same, with perhaps a minor decrease upon decreasing Pd:Cu ratio (i.e., the catalyst Pd:Cu = 1:0.33 shows slightly higher selectivity for NH_4^+ than the other Pd–Cu samples more rich in copper). On the contrary, selectivities for NO_2^- rise with decreasing Pd:Cu ratio.

The reduction of NO_2^- by H_2 addition of copper, however, does not have any beneficial influence on the catalytic activity of palladium. Moreover, as can be seen from the experimental data shown in Fig. 2, the catalytic activity (with respect to the total content of both Pd and Cu in a given sample) of the $Pd–Cu/Al_2O_3$ sample with the atomic ratio Pd:Cu = 1:0.8 (the most active in the reduction of NO_3^-) is much lower than that of Pd/Al_2O_3. Note that the activity values of Pd/Al_2O_3 and $Pd–Cu/Al_2O_3$ samples calculated with respect to the content of palladium alone are about the same — 0.33 and 0.27 mol NO_2^- mol Pd^{-1} min^{-1}, respectively.

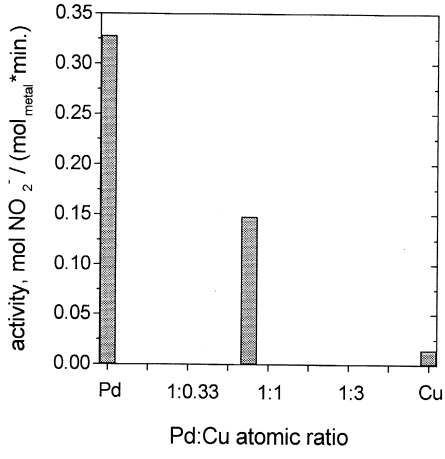

Fig. 2. Activities of Pd/Al_2O_3, Cu/Al_2O_3 and $Pd–Cu/Al_2O_3$ catalysts (mean grain size 15 μm) in reduction of nitrite ions. Reaction conditions: temperature 298 K, $P_{H_2} = 1$ bar, $C_{NO_2^-} = 50$ mg/l, pH = 6.0.

3.2. Structure of $Pd–Cu/Al_2O_3$ catalysts

Investigation of the supported catalysts by SIMS and XRD techniques was carried out to unravel the role of the metals (Pd and Cu) in the mechanism of reduction of nitrate and nitrite ions by hydrogen.

3.2.1. XRD study

The XRD data are indicative of a small size of the metal particles formed in the supported mono- and bimetallic catalysts. No peaks of palladium, copper or of their combinations (alloys) known to form in the Pd–Cu system [11–13] were detected in the XRD spectra of the reduced Pd/Al_2O_3, Cu/Al_2O_3 and $Pd–Cu/Al_2O_3$ catalysts. This is most likely due to the pronounced line broadening typical of the nanosized metal particles, along with the overlapping of the resulting halo and the peaks of the γ-Al_2O_3 support. Note that the TEM investigation of the similarly prepared Cu/Al_2O_3 catalyst showed that the size of Cu particles did not exceed 1 nm [14]. Formation of metal particles not exceeding 3–4 nm in size for the

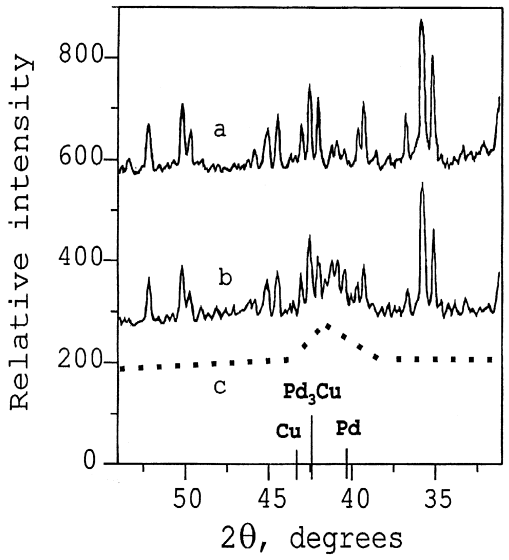

Fig. 3. XRD patterns of the catalytic membrane: diffractogram of the ceramic membrane support; diffractogram of the catalytic membrane with Pd–Cu active component; differential pattern.

supported Pd–Cu catalysts prepared via various techniques have been reported in several publications [15,16]. For the catalytic membrane containing Pd–Cu active component over the membrane support made of the natural silica–alumina mineral, XRD analysis points out the formation of nanosized bimetallic particles. Comparative analysis of XRD spectra for the membrane support and the catalytic membrane (Fig. 3) shows that the latter contains a superposition of the broad peak with the maximum at $2\theta \approx 41°$ characteristic of nanosized metal clusters and sharp peaks belonging to the membrane support. Due to the apparently small size of the metal particles and close values of interplanar distances responsible for the strongest XRD reflexes in the crystal lattices of Pd, Cu and Pd–Cu alloys, the phase composition of the metal particles cannot be accurately determined. However, it is worth mentioning that XRD patterns of the metallic particles in the catalytic membrane are similar to those reported for the silica-supported Pd–Cu catalysts in Ref. [16], where formation of palladium–copper alloys has been suggested. The Scherrer's approach based on the XRD line broadening [17] was used to calculate the mean size of the metal particles in the catalytic membrane:

$$d = \frac{\lambda}{\beta \cos\theta}$$

where λ is the wavelength of the X-ray source employed, β the semiwidth of the XRD peak of the metal particles, and θ the Bragg's angle of the peak.

At $\lambda = 0.154$ nm (CuKα radiation), $\beta = 180$ min and $\theta = 20.5°$ as it appears from the differential XRD pattern, the value $d = 3.2$ nm was obtained. Thus, on the basis of our results and those existing in the literature it can be assumed that the bimetallic Pd–Cu particles with the crystalline domains not exceeding ca. 3 nm are apparently formed on the surface of γ-Al_2O_3 and ceramic membrane supports.

3.2.2. SIMS investigation

SIMS investigation has been performed for the series of Pd–Cu/Al_2O_3 catalysts to analyse the surface composition of the *individual metal particles* deposited onto the support, as well as the concentration profile of the active component in the *porous grain* of the catalyst. The results are briefly summarised in Fig. 4.

While interpreting the data one should bear in mind that the spatial resolution of SIMS technique depends on the depth of ion etching [18,19]. Under our experimental conditions the depth resolution changes from angstroms (for

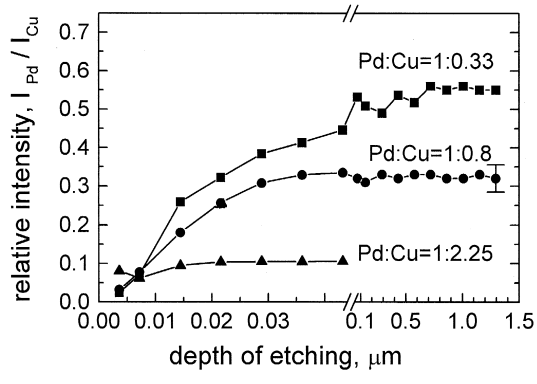

Fig. 4. Relative intensities of the ionic currents $^{106}Pd^+/^{63}Cu^+$ vs. depth of argon etching.

the initial stages of etching) to ca. 100 Å for the depth of etching of 1 μm. Therefore the dependencies of the ratios of ion currents (I) vs. depth of Ar^+ etching (Z) represented in Fig. 4, reflecting the integral composition of the catalytically active component along the *catalyst grain*, at low Z show the surface composition of the *individual metal particles* deposited on the support.

As one can see from Fig. 4, the topmost layer of the *metal particles* (catalytically active component) for the $Pd–Cu/Al_2O_3$ catalysts with the ratios Pd:Cu = 1:0.33 and 1:0.8 is strongly enriched with Cu compared to the integral bulk composition, while for the sample with the highest content of copper (Pd:Cu = 1:2.25) the composition of the metal particles apparently is more homogeneous. With the exception of the latter catalyst, the ratio Pd:Cu in the surface layer of *porous grains* of the catalysts is the lowest on the outside of a grain, gradually increasing to reach the steady level at the grain depth of ca. 0.03 μm (Pd:Cu = 1:0.8) to 0.1 μm (Pd:Cu = 1:0.33).

3.3. Interaction of H_2 with NO over Pd: TDS study

The communications on investigations of the molecular mechanism of NO_3^- and/or NO_2^- reduction by hydrogen are not known to the authors of this paper. The only exception is Ref. [20] where the hypothetical mechanism, based on the assumption that NO is the key intermediate in these reactions over noble metal catalysts [21], was suggested. Although the above assumption still needs to be proved, in the present study it was accepted as a starting point for our experimental investigations related to the mechanism of interactions between NO and H_2 over palladium. This metal was chosen as an object since it is known to be the most active amongst noble metal catalysts for the latter reaction [22]; besides, high activity and selectivity were reported for the supported palladium catalysts in the reduction of aqueous nitrite ions [2,23].

It is well known that the catalytic reaction between NO and H_2 can yield nitrogen, ammonia and nitrous oxide. Nature of the catalytic metal, reaction conditions (temperature and reactants pressures), adsorption state of NO (molecular or dissociative) dictate the particular pathway of the reaction. Thus, a partial dissociation of nitric oxide molecules on Ru at 300 K is responsible for the selective nitrogen release in the course of NO reduction by H_2, whereas on palladium and platinum NH_3 and N_2O are additionally formed [24].

A key step in the $NO + H_2$ reaction on Pd and Pt is the dissociative adsorption of NO [24]. At temperatures above 400 K, the adsorbed atoms of oxygen O_{ads} generated due to NO dissociation over the metal surface react readily with the layer of atomic adsorbed hydrogen H_{ads} to form water molecules which evolve immediately into the gas phase [8]. Recombination of N_{ads} at 500–600 K on the surface free of other species gives rise to the evolution of molecular nitrogen. Interaction of N_{ads} with NO_{ads} produces N_2O molecules; reaction between N_{ads} and H_{ads} in an excess of hydrogen at 460 K yields ammonia [25].

At lower temperatures, though, the atomized nitrogen species adsorbed over the surfaces of noble metals are quite inert. Thus, high stability of the N_{ads} layer at 300 K over Pd(110) single crystal has been found in the studies where N_{ads} was prepared via electron beam generated atomization of pre-adsorbed molecular nitrogen [26].

Thus, the problem of the low-temperature $NO + H_2$ conversion reduces primarily to a search for the optimum conditions of N_{ads} atoms formation from NO and for a prerequisite of the N_{ads} recombination into N_2 at ca. 300 K. In the present work, TDS was employed to monitor the interaction of H_2 and NO over Pd.

3.3.1. H_2 adsorption

Hydrogen adsorption has been studied in the temperature range of 100–300 K at pressures from 2×10^{-9} to 1×10^{-7} Torr. Desorption spectra recorded for palladium exposed to 0.6–

120 L (1 L = 10^{-6} Torr s) at 100 K (Fig. 5a) show two peaks corresponding to a high-temperature β-state of hydrogen (T_{des} = 350 K) and to a low-temperature α-state (T_{des} = 160 K). At the initial stage of adsorption and exposure of 1 L hydrogen is seen to fill the metal surface at the tightly bound β-state with the coverage degree close to 0.4. After exposures in the range of 60–120 L, the loosely bound α-state appears, and the saturation coverage of H_{ads} equal to 1 monolayer (θ_H = 1 ML) is reached [27]. Using the calculation procedure from Ref. [28] with the pre-exponential factor of the desorption rate constant $\gamma = 10^{13}$ s^{-1}, we obtain the activation energy values for hydrogen desorption: E^{α}_{des} kcal/mol, E^{β}_{des} kcal/mol, in good agreement with Ref. [27].

If hydrogen is adsorbed at 300 K, the desorption spectrum contains, in addition to the peak of the β-state, the high-temperature β_{ab} peak at T_{des} = 620 K that belongs to the atomic hydrogen absorbed into the bulk of palladium (Fig. 5b). Hydrogen adsorption over palladium at the conditions studied is dissociative. In our experiments this was confirmed by the total isotopic equilibration achieved in the adsorption layer that was prepared via the adsorption of a nonequilibrium H_2/D_2 mixture (50% H_2, 50% D_2) at 300 K. These results are in a good agreement with the previous studies [27,29].

3.3.2. NO adsorption

At room temperature NO adsorbs intact on Pd [24], but at higher temperatures its adsorption is expected to be accompanied by dissociation of the molecules. Evidences for the dissociative adsorption of NO are provided by our desorption experiments. Fig. 6 shows a series of desorption spectra of NO and the products of its decomposition (N_2, N_2O, O_2) obtained on Pd surface exposed to 0.3–1 L at 300 K. Nitric oxide gives a peak at 580 K at initial exposures. As NO exposure increases up to 3 L, the NO desorption spectrum exhibits a new peak at 420 K. At NO exposure of 0.2 L, N_2, desorption peaks of O_2 and N_2O appear at 700, 880 and

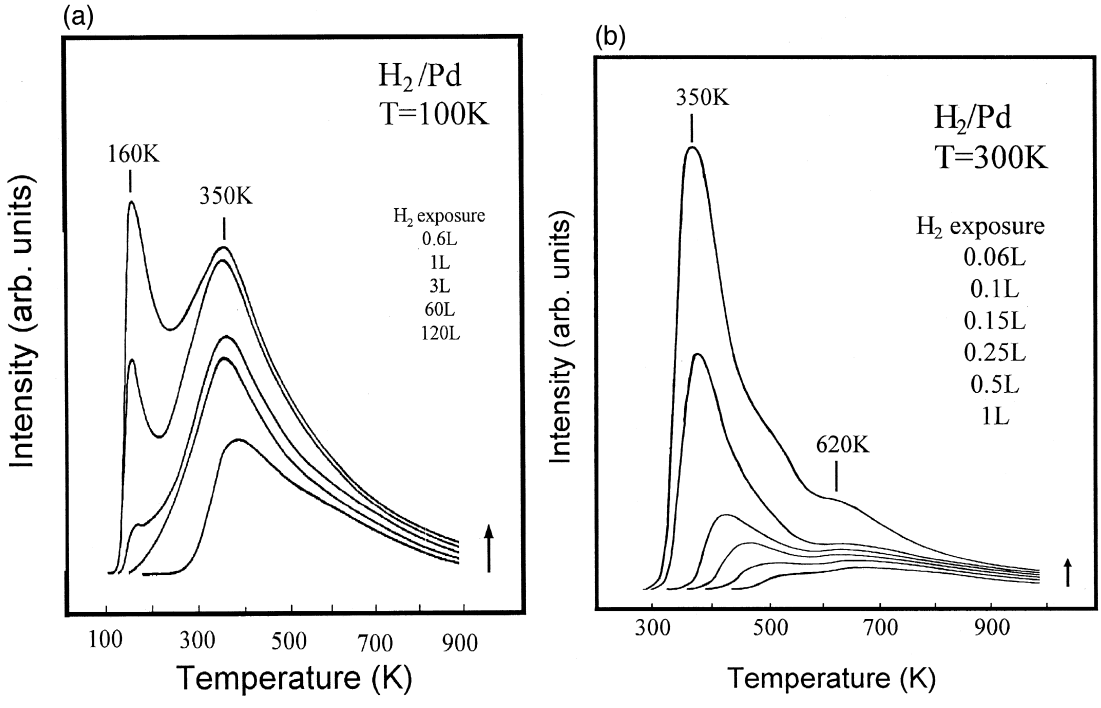

Fig. 5. Series of desorption spectra after exposure of the Pd surface to H_2 at 100 K (a) and 300 K (b).

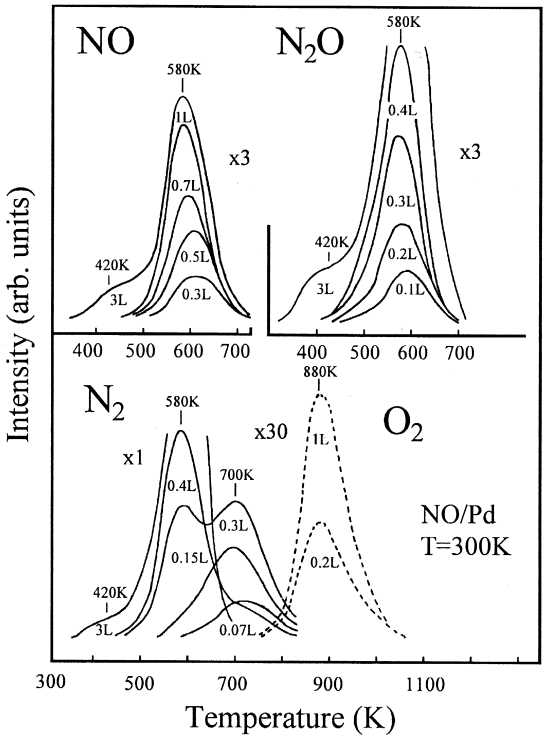

Fig. 6. Series of desorption spectra of NO, N_2, N_2O and O_2 after exposure of the Pd surface to NO at 300 K.

580 K, respectively, indicating a high dissociation probability for NO_{ads} at higher temperatures. The increase in exposure up to 1 L gives rise to a simultaneous increase in the intensity of NO, N_2O and N_2 desorptions that occur at the same temperature of 580 K, and of the O_2 peak at 880 K as well. Disappearance of the N_2 high-temperature peak at 700 K observed at exposures higher than 0.4 L is due to the population of the corresponding adsorption sites with oxygen adatoms.

3.3.3. Reaction $H_2 + NO_{ads}$

Fig. 7 shows a series of TD spectra recorded for H_2, NO and products of their reaction on Pd surface. Hydrogen is admitted into the apparatus at a pressure of $P_{H_2} = 10^{-7}$ Torr following the previous NO adsorption on the clean palladium surface at 0.3–2.5 L and 300 K. Desorption of NO upon Pd heating reveals two peaks — at 420 and 580 K. Two intensive peaks of N_2 at 580 and 680 K and two peaks of N_2O at 420 and 580 K appear due to a promoting action of hydrogen H_{ads} layer on the dissociation of NO_{ads} molecules (compare Figs. 6 and 7). A dashed curve in Fig. 7 corresponds to the hydrogen desorption at $T_{des} = 480$ K. No oxygen desorption was observed under these reaction conditions. Oxygen adatoms formed via NO dissociation are removed readily by H_2, which is accompanied by the accumulation of the tightly bound nitrogen adatoms on the vacant sites of palladium surface (the corresponding peak of nitrogen appears at 680 K). The evolution of N_2O in the gas phase observed in the presence of hydrogen indicates that the following reaction apparently occurs upon heating: $NO_{ads} + N_{ads} \rightarrow N_2O_{gas}$.

3.3.4. Reactions $NH_3 + NO_{ads}$ and $NH_3 + O_{ads}$

Fig. 8 displays a series of TDS spectra for the molecular nitrogen formed by NO_{ads} decomposition, recombination of nitrogen from the layer of nitrogen adatoms N_{ads} (the latter was produced by plasma discharge as in Ref. [30] and thereafter adsorbed over Pd), as well as for N_2 produced by the reactions $H_2 + NO_{ads}$, $NH_3 + NO_{ads}$ and $NH_3 + O_{ads}$. The reaction $NH_3 + NO_{ads}$ is being considered here since NH_3

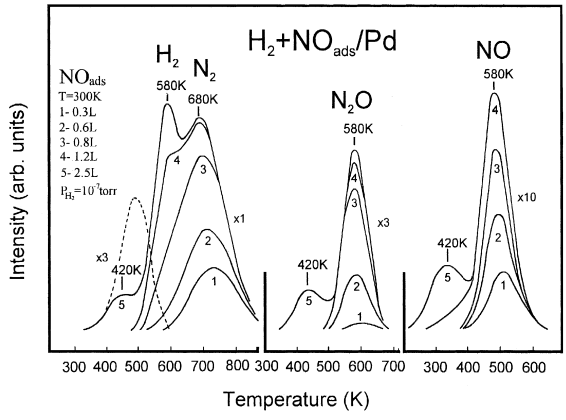

Fig. 7. Series of desorption spectra of NO, N_2, N_2O at $P_{H_2} = 10^{-7}$ Torr after exposure of the Pd surface with NO pre-adsorbed at 300 K to the reaction with H_2.

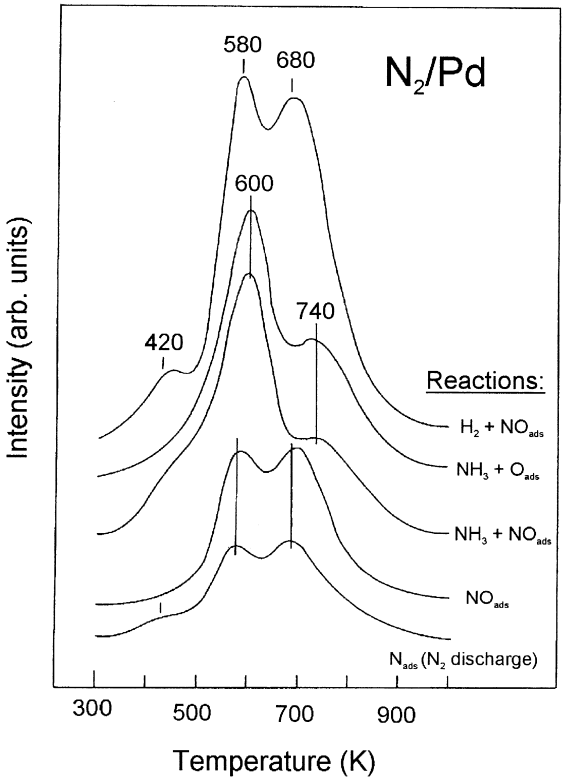

Fig. 8. Desorption spectra of N_2 from atomic nitrogen species formed on the Pd surface by (from bottom to top): (i) N_2 plasma discharge; (ii) NO dissociative adsorption; (iii) $NH_3 + NO_{ads}$ reaction at $P_{NH_3} = 2\times10^{-7}$ Torr, with NO exposure 2 L at 300 K; $NH_3 + O_{ads}$ reaction at $P_{NH_3} = 1\times10^{-8}$ Torr, with O_2 exposure 2 L at 300 K; $H_2 + NO_{ads}$ reaction at $P_{H_2} = 1\times10^{-7}$ Torr, with NO exposure 2.5 L at 300 K.

molecules that are formed in the reaction $H_2 + NO_{ads}$ [25] and that do not dissociate over Pd [24], can further interact from the gas phase with pre-adsorbed molecular nitric oxide NO_{ads} yielding nitrogen molecules. The latter can influence nitrogen coverage of the surface in the system $H_2 + NO/Pd$. Two intensive peaks of N_2 with the maximums at ca. 600 and 740 K resulting from the reaction $NH_3 + NO_{ads}$ are clearly seen in Fig. 8. The same N_2 desorption peaks (at ca. 600 and 740 K) appear in the TD spectrum due to the reaction of ammonia with the atomic surface oxygen species. In turn, the latter emerge via the surface decomposition of nitric oxide: $NO \rightarrow N_{ads} + O_{ads}$.

The data shown in Fig. 8 evidence that at least three different nitrogen surface species N_{ads} can be formed over Pd, distinguished by the thermodesorption maxima at 420, 580–600 and 680–740 K. It is likely that the concentration of N_{ads} and the strength of the Pd–N bond are the key factors determining the activity and selectivity in the $H_2 + NO$ reaction over palladium. Fig. 8 also shows that recombination of N_{ads} species is a relatively slow process at ambient temperatures. Nitrogen atoms that accumulate over Pd at these conditions can block the catalytic surface thus limiting the activity of palladium in the reaction between H_2 and NO.

4. Discussion

4.1. Reduction of NO_3^- and NO_2^- by H_2 over Pd/Al_2O_3 and Pd–Cu/Al_2O_3 catalysts

Our experimental results, in agreement with the literature data [2,21], show that the Pd/Al_2O_3 catalyst possesses relatively low activity with high yield of ammonium in the reduction of NO_3^- by H_2 in aqueous solutions. Addition of copper, by itself a poor catalyst in this reaction, gives rise to a multifold increase in the catalytic activity and considerable decrease in the yield of ammonium for Pd–Cu catalysts. It can be assumed that copper is likely to form part of the bimetallic Pd–Cu active component in this reaction. However, in the reduction of NO_2^- copper behaves as a diluent for palladium, which in the latter case seems to be the only catalytically active metal. It can be hypothesized further that these changes result from an additional route in the mechanism of NO_3^- reduction that comes into play as soon as copper is introduced in the catalyst. The surface enrichment of the supported Pd–Cu particles in copper, registered for our catalysts and membranes in line with numerous observations reported in the literature [15,31–35], together with an increase in the catalytic activity obtained

upon addition of copper to palladium also suggests that it is probably not the activation of hydrogen but that of NO_3^- which is the rate-limiting step for the palladium-based catalysts.

4.2. Investigation of the mechanism of NO_3^- and NO_2^- reduction by H_2

4.2.1. The nature of hydrogen adsorbed over Pd

Of the Group VIII metals it is only palladium that reacts with hydrogen to form a stable hydride phase. The solubility of hydrogen in the bulk of palladium is abnormally high, and the three-dimensional phase of palladium hydride can be formed at various P_{H_2} and temperature. Palladium hydride is likely to be formed in the course of H_2 adsorption, which is evidenced by the TDS results presented in Fig. 5a–b. The dissociative state of hydrogen produced under adsorption at 300 K is characterized by the high-temperature β peak at 350 K ($\theta = 0.4$ ML), whereas hydrogen adsorption below room temperature results in the low-temperature α peak at 160 K. The latter only appears after large exposures at 100 K and exhibits near-zero-order desorption kinetics [9]. The α peak is associated with a near-surface hydrogen state and, therefore, can be assigned to the decomposition of surface hydride. According to Ref. [36], the hydride phase has an atomic ratio $H/Pd \geq 0.6$. Hence, the low-temperature formation of the surface hydride is caused by (i) high coverage θ_H, (ii) slow hydrogen diffusion into the bulk. A high diffusion rate of hydrogen in Pd at 300 K (3.8×10^{-7} cm^2 s^{-1}, which corresponds to the movement speed of 2×10^{-4} mm/s) results in the appearance of the wide desorption β_{ab} peak at 620 K, in accordance with Refs. [29,36]. Hydrogen can also diffuse in the bulk of palladium in the course of the reaction between NO and H_2. As evidenced by the HREELS study [37], the NO adlayer forces hydrogen atoms to move deeper into the substrate. Thus, the three characteristic TDS spectra for the H/Pd system (α, β and β_{ab}) are strongly dependent on the adsorption temperature and exposure, or the reaction conditions (i.e. temperature and partial pressures of the reactants).

4.2.2. NO dissociation and NO + H_2 interaction over Pd

The adsorption of NO on Pd at 300 K is predominantly molecular. It occurs via nitrogen binding to Pd. Upon heating, a portion of NO desorbs reversibly from Pd, but the residual NO dissociates releasing N_2, O_2 and N_2O in addition to NO (Fig. 7). This implies that the thermal decomposition of NO occurs more readily on the polycrystalline palladium wire as compared with the flat Pd(111) and Pd(100) surfaces [24,38]. The fractional amount of NO dissociation on the polycrystalline surface upon heating is the largest at the lowest NO coverages, when only defect sites are populated with NO_{ads}. However, the dissociation probability diminishes steeply when the surface defect sites become populated with O_{ads} atoms, and the high-temperature peak with $T_{max} = 700$ K disappears.

When NO adsorbs dissociatively on Pd surface in the presence of hydrogen at 300 K, oxygen atoms thus formed are readily removed by hydrogen to form H_2O, while the adsorbed atomic nitrogen species remain on the surface (in the equations below, square brackets symbolise the active surface centers):

$$H_2 + 2Pd[] \rightarrow 2Pd[H] \quad (1)$$

$$Pd[NO] + Pd[] \rightarrow Pd[N] + Pd[O]$$

$$Pd[O] + 2Pd[H] \rightarrow 3Pd[] + H_2$$

$$Pd[NO] + H_2 \rightarrow Pd[N] + H_2O$$

According to Ref. [39], if recombination of N_{ads} is rapid under the reaction conditions, then only a slight accumulation of N_{ads} would be attained. It has been also found in Ref. [39] that N_2 desorption from the layer of atomic nitrogen is slow for Pd(100) surface, and the N_{ads} layer is stable at temperatures below 600 K in vacuum. As shown in Fig. 8, the growth in the N_{ads} coverage is apparently associated with the

species desorbed at ca. 680 K. For the $N_{ads} + H_2$ reaction on Pd(100) at 400 K, the formation of NH_{ads} species — an intermediate in the reaction pathway leading to ammonia production — has been observed in Refs. [25,39].

4.2.3. Mechanism of NO reduction by H_2 over Pd

In our study attention was focused at transformations of NO (the probable key intermediate in reduction of NO_3^- and NO_2^-) occurring over Pd and leading to the main reaction products — N_2 and NH_3. In the light of the present study and the data available in the literature, formation of nitrogen via the surface decomposition of NH_{ads} species as suggested in Ref. [20], i.e. $2NH_{ads} \rightarrow N_2 + 2H_{ads}$ is unlikely to take place under conditions of NO_3^- and/or NO_2^- reduction over Pd. A similar reaction resulting in the simultaneous evolution of nitrogen and hydrogen in the gas phase can occur over Ir [40] and Rh [41] surfaces, but only at elevated temperatures. In accordance with the data existing in the literature [7], the present study shows that the main pathway of N_2 formation in the course of reduction of nitrate and/or nitrite ions over Pd is likely to include the following sequence of elementary steps:

$$\begin{aligned} &Pd[NO] + Pd[] \rightarrow Pd[N] + Pd[O] \\ &Pd[O] + 2Pd[H] \rightarrow 3Pd[] + H_2O \\ &Pd[N] + Pd[N] \rightarrow 2Pd[] + N_2 \end{aligned} \quad (2)$$

Besides, no experimental evidence can be found for the formation of NH_{ads} species over Pd via direct interaction of NO_{ads} and $2H_{ads}$, suggested in [20], i.e. $NO_{ads} + 2H_{ads} \rightarrow NH_{ads} + OH_{ads}$. As shown in the previous section, in the interaction of NO and H_2 over Pd no immediate formation of any species containing both nitrogen and hydrogen was registered. Instead, interaction between NO_{ads} and H_{ads} includes dissociation of NO_{ads} that produces N_{ads} and O_{ads} species, while NH_{ads} is formed via the surface reaction between N_{ads} and H_{ads}.

4.2.4. Mechanism of NO_3^- and NO_2^- reduction by H_2 over Pd and Pd–Cu catalysts

On the basis of the results obtained in this study and the literature data, the following mechanism of NO_3^- and NO_2^- reduction by hydrogen in aqueous solutions over Pd and bimetallic Pd–Cu catalysts can be proposed:

$$\begin{aligned} &(1)\ H_2 + 2Pd[] \rightarrow 2Pd[H] \\ &(2)\ NO_3^- + Pd[H] \rightarrow Pd[NO_2] + OH^- \\ &(3)\ Pd[NO_2] \Leftrightarrow NO_2 + Pd[] \\ &(4)\ 2NO_2 + 2OH^- \rightarrow NO_2^- + NO_3^- + H_2O \\ &(5)\ NO_2^- + Pd[H] \rightarrow Pd[NO] + OH^- \\ &(6)\ Pd[NO_2] + Pd[H] \rightarrow Pd[NO] + Pd[OH] \\ &(7)\ NO_3^- + 2Cu[] \rightarrow [Cu_2O]_{surf} + NO_2^- \\ &(8)\ [Cu_2O]_{surf} + 2Pd[H]_{spil} \\ &\quad \rightarrow 2Cu[] + 2Pd[] + H_2O \\ &(9)\ Pd[NO] + Pd[] \rightarrow Pd[N] + Pd[O] \\ &(10)\ Pd[O] + 2Pd[H] \rightarrow 3Pd[] + H_2O \\ &(11)\ Pd[N] + Pd[N] \rightarrow 2Pd[] + N_2 \\ &(12)\ Pd[N] + Pd[H] \rightarrow Pd[NH] + Pd[] \\ &(13)\ Pd[NH] + Pd[NH] \rightarrow N_2 + H_2 + 2Pd[] \\ &(14)\ Pd[NH] + Pd[H] \Leftrightarrow Pd[NH_2] + Pd[] \\ &(15)\ Pd[NH_2] + Pd[H] \rightarrow Pd[NH_3] + Pd[] \\ &(16)\ Pd[NH_3] \rightarrow NH_3 + Pd[] \\ &(17)\ NH_3 + H_2O \rightarrow NH_4^+ + OH^- \\ &(18)\ Pd[OH] + Pd[H] \rightarrow H_2O + 2Pd[] \end{aligned} \quad (3)$$

In this mechanism an important role belongs to the active centers of copper which in addition to those of palladium apparently take part in the catalytic cycle of NO_3^- reduction, increasing the overall reaction rate and decreasing the yield of NH_4^+ by-product as evidenced by the kinetic measurements with Pd/Al_2O_3 and $Pd–Cu/Al_2O_3$ catalysts. Upon interaction with NO_3^- copper is likely to act as an oxygen scavenger, forming the surface oxide of the probable composition $Cu_2O_{(surf)}$ [42] and reduc-

ing the nitrate ion to NO_2^-. Besides, the atoms of metallic copper adjacent to the atoms of palladium could compete with Pd[H] species and Pd[ ] vacant sites participating in the reductions of the surface species Pd[NO_2] and Pd[NO] suggested by stages (6) and (9). The surface copper oxide $Cu_2O_{(surf)}$ thus formed is reduced back to the metallic state by hydrogen spilt-over from the adjacent Pd centers. Evidences of hydrogen transfer from palladium to copper via spillover have been found for Pd–Cu catalysts in Ref. [42]. Dissociative adsorption of hydrogen over Pd–Cu catalysts at the conditions of NO_3^- reduction can only occur on palladium sites [43,44]. It seems likely that activation of NO_3^- ion is slow for palladium, while it easily occurs over copper where nitrate ions are reduced to nitrites. This new route opened by copper is believed to account for the substantially higher activity of $PdCu/Al_2O_3$ catalysts in NO_3^- reduction compared to that of Pd/Al_2O_3. In addition to the new reaction pathway opened by the copper centers, changes in the catalytic behavior of Pd–Cu catalysts may arise from the differences in the binding energies of the adsorbed species for mono- and bimetallic systems which may result from an electronic interaction between Pd and Cu [11,43].

With the exception of stages (7) and (8), the same sequence of equations can be suggested to describe the reaction mechanism over Pd catalyst. In this case the main difference between mechanism (3) and that proposed in Ref. [20] concerns the stages of nitrogen formation, which are supposed to follow the above-given scheme (2). Since the intrinsic catalytic activity of copper in reduction of NO_2^- is low, it can be assumed that the reductive transformations of NO_2^- mainly occur over palladium.

5. Conclusion

The catalytic behavior of mono- and bimetallic catalysts with Pd and/or Cu supported over γ-Al_2O_3 in the reduction of aqueous nitrate and nitrite ions by hydrogen was investigated. Activity of the catalysts in the reduction of nitrates was found to reach maximum at the atomic ratio of the metals Pd:Cu $\approx$ 1. In the reduction of nitrite ions over the same catalysts, maximum activity was registered for Pd/Al_2O_3 catalyst, with copper apparently playing the role of an inert diluent for palladium. The composition of the supported metal catalysts was analysed using SIMS and XRD techniques. Surface enrichment in copper of the nanosized bimetallic particles (catalytically active component) was revealed. Interactions of H_2 and NO (probable intermediate in NO_3^- and NO_2^- reduction) over Pd were studied by the thermal desorption spectroscopy technique. Molecular mechanism of NO_3^- and NO_2^- reduction by H_2 over Pd and Pd–Cu catalysts is proposed.

Acknowledgements

Financial support of the investigations related to this article provided by the Netherlands Organization for Scientific Research (Grant No. 047-010-100-96) and Russian Foundation for Basic Research (Grant No. 99-003-32433) is gratefully acknowledged.

Sincere gratitude is addressed to Dr. B.E. Nieuwenhuys for the insightful discussions of mechanistic aspects of the reactions considered in the present study.

References

[1] K.-D. Vorlop, T. Tacke, M. Sell, U.S. Patent 4 990 266 (1989).
[2] K.-D. Vorlop, T. Tacke, Chem.-Ing.-Tech. 61 (1989) 836.
[3] O.M. Ilinitch, F.P. Cuperus, L.V. Nosova, E.N. Gribov, Catal. Today 56 (2000) 137–145.
[4] V.I. Nefedov, V.T. Cherepin, Physical Methods of Investigation of Solid Surfaces, Nauka, Moscow, 1983, (in Russian).
[5] G. Verner, in: Electronic and Ionic Spectroscopy of Solid Bodies, Mir, Moscow, 1981, p. 345, (in Russian).
[6] G. Bets, G. Verner, in: Sputtering of Solid Bodies by Ionic Bombardment, Mir, Moscow, 1986, p. 24, (in Russian).
[7] A. Obuchi, S. Naito, T. Onishi, K. Tamaru, Surf. Sci. 122 (1982) 235.

[8] E.M. Stuve, S.W. Jorgensen, R.J. Madix, Surf. Sci. 146 (1984) 179.
[9] M. Milun, P. Pervan, K. Wandelt, Surf. Sci. 189/190 (1987) 466.
[10] A.W. Aldag, L.D. Schmidt, J. Catal. 22 (1971) 260.
[11] Y. Debauge, M. Abon, J.C. Bertolini, J. Massardier, A. Rochefort, Appl. Surf. Sci. 90 (1995) 15.
[12] F. Skoda, M.P. Astier, G.M. Pajonk, M. Primet, Catal. Lett. 29 (1994) 159.
[13] F. Skoda, M.P. Astier, G.M. Pajonk, M. Primet, React. Kinet. Catal. Lett. 55 (1995) 101.
[14] L.N. Nosova, V.I. Zaikovskii, Yu.A. Ryndin, React. Kinet. Catal. Lett. 53 (1994) 131.
[15] L.V. Nosova, V.I. Zajkovsky, A.V. Kalinkin, E.P. Talzi, E.A. Paukshtis, Yu.A. Ryndin, Kinet. Katal. 36 (1995) 362, (in Russian).
[16] A.J. Renouprez, K. Lebas, G. Bergeret, J.L. Rousset, P. Delichere, Supported Pd–Cu catalysts prepared from bimetallic organo-metallic complexes: relation between surface composition measured by ion scattering and reactivity, in: J.W. Hightower, W.N. Delgass, E. Iglesia, A.T. Bell (Eds.), Stud. Surf. Sci. Catal. Vol. 101 Elsevier, Amsterdam, 1996, pp. 1105–1114.
[17] L.I. Mirkin, in: Analysis of Polycrystals by X-ray Diffraction, Fizmatgiz, Moscow, 1961, p. 728, (in Russian).
[18] S. Hoffman, Surf. Interface Anal. 2 (1980) 148.
[19] C.P. Hunt, M.P. Seach, Surf. Interface Anal. 5 (1983) 199.
[20] J. Wärna, I. Turunen, T. Salmi, T. Maunula, Chem. Eng. Sci. 49 (24B) (1994) 5763.
[21] S. Hörold, K.-D. Vorlop, T. Tacke, M. Sell, Catal. Today 17 (1993) 21.
[22] T.P. Kobylinski, B.W. Taylor, J. Catal. 33 (1974) 376.
[23] A. Pintar, G. Berčič, J. Levec, AIChE J. 44 (1998) 2280.
[24] W.F. Egelhoff, in: D.A. King, D.P.N.Y. Woodruff (Eds.), The Chemical Physics of Solid Surface and Heterogeneous Catalysis Vol. 4 Elsevier, Amsterdam, 1982, p. 397.
[25] T. Yamada, K. Tanaka, J. Am. Chem. Soc. 111 (1989) 6880.
[26] Y. Kuwahara, M. Fujisawa, M. Jo, M. Onchi, M. Nishijima, Surf. Sci. 188 (1987) 490.
[27] A.W. Aldag, L.D. Schmidt, J. Catal. 22 (1971) 260.
[28] P.A. Redhead, Vacuum 12 (1962) 203.
[29] H. Conrad, G. Ertl, E.E. Latta, Surf. Sci. 41 (1974) 435.
[30] K. Schwaha, E. Bechtold, Surf. Sci. 66 (1977) 383.
[31] A.D. Langeveld, H.A.C.M. Hendrickx, B.E. Nieuwenhuys, Thin Solid Films 109 (1983) 179.
[32] A. Noordermeer, G.A. Kok, B.E. Nieuwenhuys, Surf. Sci. 172 (1986) 349.
[33] D.J. Homes, D.A. King, C.J. Barnes, Surf. Sci. 227 (1990) 179.
[34] M.A. Newton, S.M. Francis, Y. Li, D. Law, M. Bowker, Surf. Sci. 259 (1991) 45.
[35] A. Rochefort, M. Abon, P. Delichère, J.C. Bertolini, Surf. Sci. 294 (1993) 43.
[36] G.E. Gdowski, T.E. Felter, R.H. Stulen, Surf. Sci. 181 (1987) L147.
[37] C. Nyberg, P. Uvdal, Surf. Sci 211/212 (1989) 923.
[38] R.D. Ramsier, Q. Gao, H.N. Waltenburg, K.W. Lee, O.W. Nooij, L. Lefferts, J.T. Yates Jr., Surf. Sci. 320 (1994) 209.
[39] K. Tanaka, T. Yamada, B.E. Nieuwenhuys, Surf. Sci. 242 (1991) 503.
[40] V.V. Gorodetskii, V.A. Sobyanin, in: Proc. VII Int. Congr. Catalysis, Tokyo Press, University of Tokyo, Tokyo, 1980, p. 566.
[41] A.R. Cholach, M.F.H. van Tol, B.E. Nieuwenhuys, Surf. Sci. 320 (1994) 281.
[42] C.A. Leon y Leon, M.A. Vannice, Appl. Catal. 69 (1991) 291.
[43] A. Rochefort, M. Abon, P. Delichère, J.C. Bertolini, Surf. Sci. 294 (1993) 43.
[44] C.A. Leon y Leon, M.A. Vannice, Appl. Catal. 69 (1991) 269.